Spring 01 Jan 2022

# AM surface roughness and its impact on drag

Jackson Landry Chandler

# AM SURFACE ROUGHNESS AND ITS IMPACT ON DRAG

by

JACKSON LANDRY CHANDLER

A THESIS

Presented to the Graduate Faculty of the

MISSOURI UNIVERSITY OF SCIENCE AND TECHNOLOGY

In Partial Fulfillment of the Requirements for the Degree

BACHELORS OF SCIENCE WITH HONORS IN AEROSPACE AND MECHANICAL ENGINEERING

April 20, 2022

Approved by:

Kelly Homan, Advisor
Phillip Bode
David J Westenberg
Nancy J. Stone
Larry Dale Gragg

# ABSTRACT

The main goal of this thesis is to quantify additive manufacturing (AM) surface roughness, as a precursor to identifying its impact on unsteady transient flow properties. Experimental data using the Hirox optical microscopes and SEM imaging collected from the nylon and stainless-steel lattice structures contained an inherent level of surface roughness at the finer scale. Surface Roughness have a negative effect on additively manufactured materials and as such should be mitigated whenever possible. Surface roughness increases unwanted features such as the level of drag, skin friction, negative heat transfer/mass transfer properties, and other unwanted unsteady transitional flow characteristics. Though exceptions may exist for surface roughness either having very little adverse effects or improving flow characteristics such as those seen on riblet designs, undesigned surface roughness features should be avoided whenever possible. From the data taken from this experiment, an additional step in research should be implemented so that more analysis can be obtained on unsteady transitional flow characteristics using constant temperature anemometry (CTA) as used in measurements of turbulent gas flows.

# TABLE OF CONTENTS

# 1. INTRODUCTION

The main goal of this thesis is to quantify additive manufacturing (AM) surface roughness, as a precursor to identifying its impact on unsteady transient flow properties. In additive manufacturing, there has been a rapid development in both materials and geometric complexity that can be fabricated. As such, there is now the potential to produce surface geometries which produce unique flow behaviors and, accordingly, beneficial surface transport (heat and mass transfer). Practically, fluids are known to be quite sensitive to both large-scale and small-scale geometric details. Compared to traditional surfaces, additively manufactured surfaces have much flexibility on the large-scale details, however, they have an inherent level of roughness at the fine scale.

In this present research, investigations in the use of traditional metallographic techniques and SEM imaging to measure the surface roughness of AM-fabricates lattice structures will be performed. This will be done by measuring representative geometry lattice structures composed of 1x1 in. nylon and stainless-steel samples that have been fabricated as part of a current research project, with consumables available in the PI/Instructor lab and SEM available at the Missouri S&T metallurgy labs. The methodology will be to encapsulate the lattice structure into an epoxy mold, cut the samples, polish the samples to smooth them, and finally to observe the characteristics of the lattice structure through both optical microscopes and SEM imaging. These images will then be processed with an open-source software as to determine the roughness of the material from the collected images. Correlations can then be made from the experimental data to literature performed by author researchers.

## 2. LITERATURE REVIEW

The literature review presents a general overview on the trends in additive manufacturing surface roughness and the impact that surface roughness has on drag and other aerodynamics forces. In addition, to use this research to perform analysis on AM surfaces for nylon and steel lattice structures.

For clarification, surface roughness is a measure of the texture of a surface. This is measured in vertical deviations of how the surface is against how it should look. With a low surface roughness, a surface is smooth, but with a high surface roughness a surface is uneven. Values for surface roughness are measured as a high-frequency, short-wavelength component and both amplitude and frequency are needed to ensure that a surface is fit for usage (**Roughness Measurements of Stainless-Steel Surfaces**). While that may not matter much depending on the application, many components whether that's for gear boxes, heat transfer systems, bearings, etc. requires a certain level of smoothness to operate efficiently. Especially since 3D printed parts have inherently greater surface roughness than CNC machining, casting, or metal injection molding. The rougher the surface in an integrated system, the less efficient, quiet, and safely they'll operate. In other words, based on the results obtained from the papers, properties of polished surfaces, or at least surfaces with consistent and uniform surface roughness, are better than unpolished, jagged, samples.

This is seen in a study on AlSi10Mg alloy produced by Selective Laser Melting (SLM) showed that corrosion resistance and corrosion fatigue endurance were improved for the polished samples (**Avi Leon, Eli Aghion**). In a study over modeling Selective Laser Sintering (SLS) and its effects on surface roughness an increase in laser power

reduces surface roughness, scan spacing from a low level up toward a central level decrease surface roughness but then increases afterwards, and an increase in hatch length decreases surface roughness. For instance, starting at pre sintered SLS parameters ($R_z \; and \; R_a$), the top surface roughness was $R_z = 35 - 45$ µm $and \; R_a = 10 - 12$ µm. This is compared to optimized operational conditions were surface roughness reduced to $R_z = 33.2$ µm $and \; R_a = 6.9$ µm. As such, a strong correlation between the laser power, scan spacing, and bed temperature has a great influence on the surface roughness of a material (**Sacheva, Anish, et. al**). Additionally, another paper by **Fox, Jason C., et. al** studying surface roughness of overhang structures in laser powder bed fusion for powders of 20-100 µm states that for peak counts and mean width/heights of profile elements indicates a shift controlled by partially melted powder particles (seen at lower powers) and those dominated by re-solidified melt track (seen at higher powers). While the paper by **Sacheva, Anish, et. al** argued that plasma power was the most significant influence on surface roughness. **F. Calignano, et. al** studied aluminum parts (ALSi10Mg) produced by direct metal laser sintering (DMLS) and they stated that scan speed had the greatest influence. Additionally, shot peening was indicated to effectively improve surface roughness qualities. With optimal parameters of a scan speed 900 mm/s and a laser power of 120 watts. In addition, for one sample of aluminum, staring at a surface roughness of 23.95 µm and applying a pressure of 4 bars and 8 bars, the shot peening reduced this down to 13.78 µm and 5.85 µm, respectively. Meaning that an increase in pressure for shot peening, leads to a reduction in surface roughness.

Therefore, inconsistent surface finishing and unpredictable workflow is demonstrated when manual surface finishing or semi-automated manufacturing

equipment is used. That is why a more digitized, diligent, and automated approach for uniform surface finishing must be employed for consistent mass heat transfer characteristics and air flowability. Additionally, texture characterization of these additively manufactured surfaces is highly important in the early stages of development for better understanding of a products capabilities and identifying a correlation for a component's functional performance (**Townsend, A, et. al**).

Surface Roughness, as one may imagine, can have a drastic and often undesirable effect on aerodynamic drag and skin friction occurring on the surface of a material. In a study by **Rajappan, Anoop, et al.** a large autocorrelation length, a small surface roughness, and a presence of hierarchical roughness features as being three of the most important design requirements for achieving optimal drag reduction in turbulent flows for scalable superhydrophobic textures. This is seen in a study by **Ketut Aria Pria Utama, et. al**. over a study on the skin friction drag of a freshly cleaned and painted ship hull. From their results it states seemingly minute roughness (0.1-0.5 mm in physical height) can cause an estimated 31% increase of skin-friction drag compared to a surface that is hydrodynamically smooth. This suggests that more careful cleaning and painting procedures are needed to lower drag penalty. The main reason for this is the surface roughness causing turbulent boundary layers forming over the ship's hull and causing energy consumption in ocean fairing endeavors. The researchers even estimate that 80-90% of the total drag experienced by a bulk carrier is precisely due to this turbulent skin-friction drag dilemma.

Similar results were seen by **Ehrmann, Robert S., et.** al from Sandia National Laboratories on the on the "Effect of Surface Roughness on Wind Turbine Performance".

With an increase in both distributed roughness height and density increase, the lift-curve slope, lift-to-drag ratio, and maximum lift all decrease. For instance, at a Reynolds number of $3.2 * 10^6$ had a maximum lift-to-drag ratio decrease of 40.8% for 140 micrometers. This causes a 2.3% loss in annual energy production. Another interesting metric found from this paper is that by using 25%, 30%, 35%, and 40% thick airfoils with trip-strip (meaning attaching strips at 45 degrees) roughness, the airfoils with 25% and 30% thickness were less sensitive to compared to 35% and 40% thick airfoils. This means that as airfoils grow thicker, roughness sensitivity and "insect accumulation" increases. As such, finding ways to reduce annual energy production by reducing the surface roughness of wind turbine blades are better for finding better ways to use cost effective blade maintenance metrics.

Skin-friction, roughness functions and other predictive correlations were displayed in a paper by **Flack, K. A., et. al** to determine the role of roughness on amplitude and skewness of studied materials. Root-mean-square (rms) roughness height and skewness of the probability density function were used to investigate these parameters in generating friction at the wall. Results showed that negative skewness (pits) had a much smaller influence on drag than the positive skewness (peaks) did. The papers states that most of the surfaces can be predicted down to a single roughness function in a transitionally rough surface regime like the one found by **Nikuradse (1933)** for uniform sand-grain roughness. However, exceptions exist for wavy surfaces and a surface with high positive skewness. More specifically wavy surfaces with an effective slope of less than 0.35 (Effective slope is defined as $ES = \frac{1}{L_s}\int |\frac{dr}{dx}| dx \ \ where \ L_s$ is the sampling length, r is roughness amplitude, and x the streamwise direction) and highly

skewed surfaces require different or additional parameters. Similar results were found from some of the same previous authors **Flack, Karen A., et. al** over a systematic change in the surface roughness skewness on turbulence and drag. With the roughness heights fixed, the ratio of heights to boundary layer thickness changed modestly because of an increase in boundary layer thickness from the skewness change from negative to positive. From both papers, it seems that roughness skewness is an important parameter for predicting drag. This is especially the case for materials with a close packed roughness. As such, skewness, in conjunction with surface height and surface slope are helpful in predicting surface drag.

Though it is interesting to point out one paper by **Barros, Julio M., et. al** over the "measurements of skin-friction of systematically generated surface roughness" utilized a fixed amplitude varying power-law spectral slope ($E(\kappa) \sim \kappa^P$, P = -0.5, .1.0, and 1.5) were used for 3d printing. The power slopes essentially changing the slopes at which the surface roughness changes with respect to the surface (See **Fig.1**). Results showed that the surface with a shallower spectral slope (P = -0.5) had the highest drag whereas the surface with a steeper slope (P = -1.5) had the least drag. This is even though the 3d printed part with P = -0.5 had the smallest surface roughness features of the three samples. As such, as the power law slope increases, the drag imposed by the surface is reduced. This is speculated due to the undulating wavy surface features of the 3d printed material and that surface wavelengths are not a significant contribution to the drag.

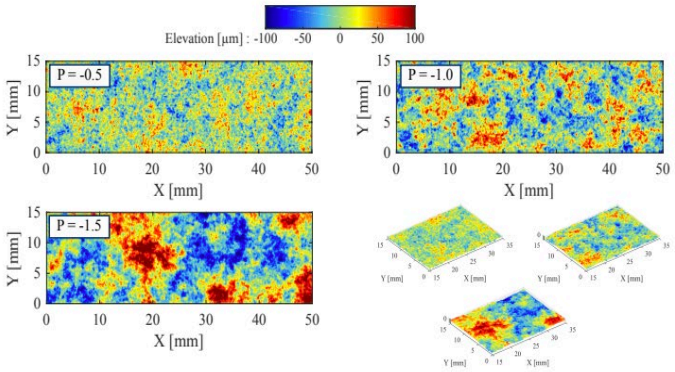


**Figure 1: Contour maps of the printed version from the mathematically generated rough surfaces with power law slope P = -0.5, -1.0, and -1.5**

Though one should bear in mind that for certain applications, the addition of varying surface roughness may prove beneficial. This can be seen on **Abbas, A. A., et. al** study on the "Surface Roughness Effects on Turbulent Boundary Layer Structure of NACA 0026 Airfoil". The airfoil has a geometry of 500 mm span, 600 mm chord, and 156 mm maximum thickness. An application of riblets (essentially microscale jagged teeth that are formed along the direction of air flow) is seen to affect boundary layer properties on the airfoil (See **Fig. (2-3)** for images of riblets). At a Reynolds number of 200 and a freestream velocity of 5 m/s the riblets causes the boundary layer and turbulence intensity profiles to match closely with a favorable pressure gradient. Without said riblets, the flow has a very small layer of logarithmic region and high wake (within the velocity profile) with a highly energized inner region (within the intensities profiles)

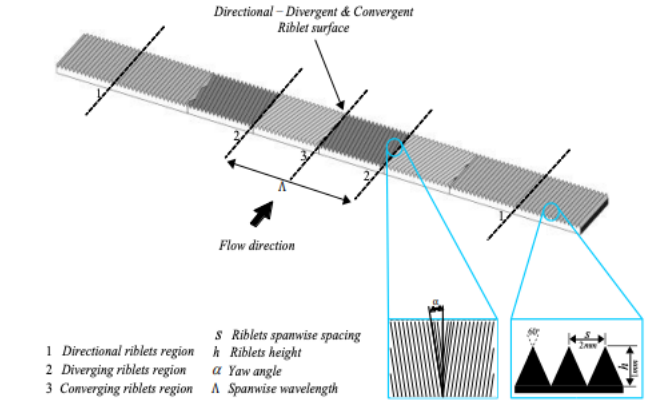


**Figure 2: Schematic Diagram Showing the key dimensions of herringbone Surface Type – Riblets (directional – diverging and converging pattern) with the details for the cross-sectional area of the riblets strips**

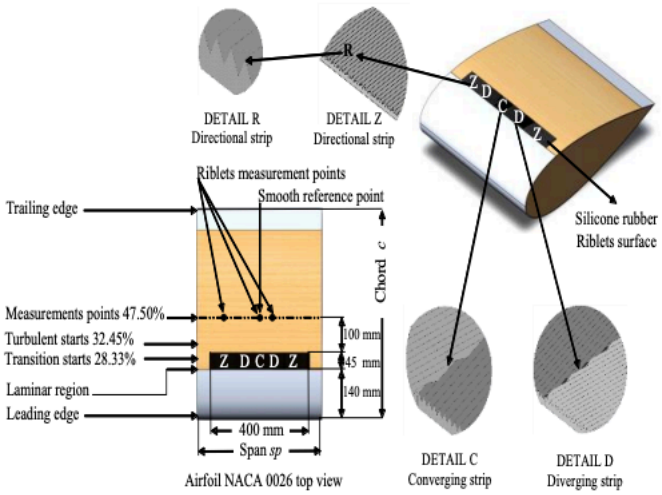


**Figure 3: Schematic diagram of a NACA 0026 airfoil showing the dimensions and application of riblet in black strip, the location of transition, the start of turbulent, and the measurements points for both smooth and riblet surfaces boundary layer in chord percentage**

Similar results for riblets are seen in a study by **Harun, Zambri, et al.** over the effects that surface roughness has on transportation industries. Aerodynamic forces and skin friction effects, at least according to the researchers, are the two main deciding factors for changes in fuel efficiencies. With skin friction causing the majority of drag

within a streamlined body (especially tankers). As mentioned in the previous study by **Abbas, A. A., et. al**, riblets can help reduce the drag effects on a super tanker and thereby alters the overall ship's fuel consumption intake. Though it should be mentioned that for this study, there has not been much conclusive results as turbulent flows over rough surfaces is a research topic that needs much more data acquisition and research. As varying applications and surface roughness functionality and design considerations vary wildly and causes different aerodynamic and skin friction effects. However, a safe assumption to make is that surface roughness features that were not intentionally created almost always tends to create undesirable results.

# 3. EXPERIMENTAL PROCEDURE

## 3.1. SAMPLE PREP

In this experiment, epoxy mixing cups of approximately 1.5” diameter, epoxy resin (Leco 811-563-107 used at Missouri S&T), Hardener (Leco 811-563-107 used at Missouri S&T), grinding pads (see **Section 3.3**), and a precision saw blade (Wafering Blades – Solid Core – Resin Bond) are to be used. This will be used to start analysis on analysis surface roughness features on two sets of materials of 1”x1”x1”, which are stainless steel and nylon (**See Fig. (4))** for example of a lattice structure).

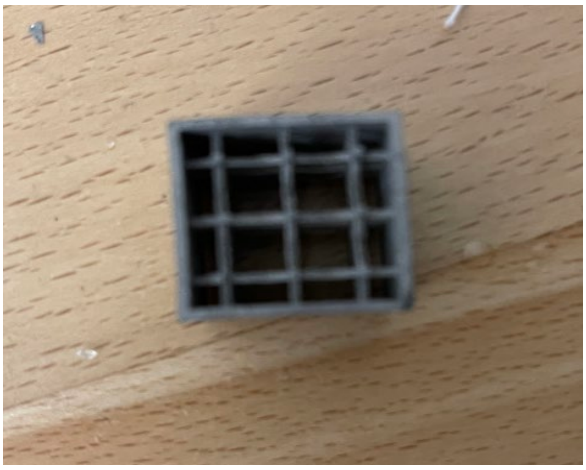

**Figure 4: Lattice Structure of Stainless Steel**

## 3.2. SAMPLE ENCAPSULATION

Next the lattices on the outer sides should be marked where the saw cut should be made. This is so that the saw gets as close to the latices as possible without hitting the edges. Two to three pieces can be obtained from each structure. The samples should then be placed in epoxy resin by performing the following steps:

a) Place the sample in a mixing cup (1.5”) with the open sides of the cube perpendicular to the surface of the mounting cup.

b) Mix a 5:1 ratio of epoxy to hardener with an ideal amount of 3 grams of hardener per sample and 15 grams of epoxy per sample. Make sure the mixture does not overfill within the mounting cup

c) Mix the solution until the bubbles are visible gone and the solution starts to become clear.

d) Then the solution is to be poured into the mixing cups and completely covering the sample.

e) Then the samples are to be placed in a vacuum chamber (SP Science Ware) powered by a vacuum pump (Kozyvacu Model TA450) for approximately 10-20 minutes, until all the bubbles have left the surface of the epoxy. But be sure to not set the pressure level down to quickly or else the epoxy resin mixture will spill over inside of the vacuum chamber. Always keep an eye on the vacuum chamber during this step. (**See Fig. (5)**).

f) Let the samples sit in the vacuum chamber sit for 4 to 5 hours before removing from the mixing cups.

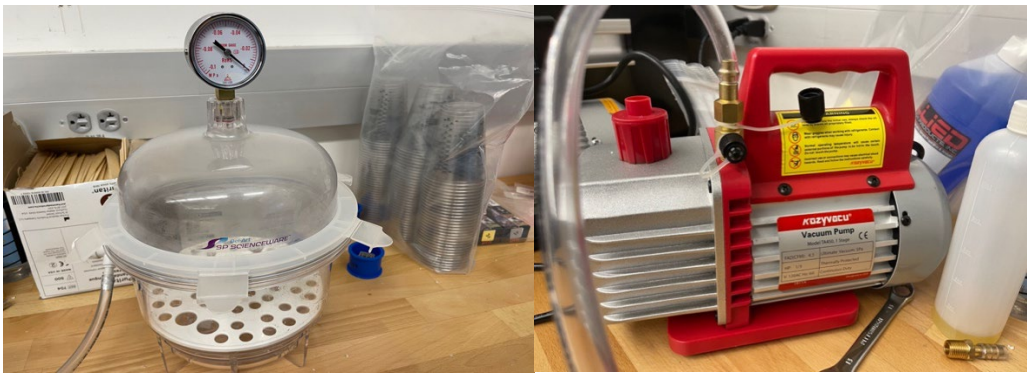


**Figure 5: Vacuum Chamber (left) and Kozyyacu Vacuum Pump (right)**

### 3.3. CUTTING AND POLISHING

After removing the samples from the mounting caps, the precision saw was used to cut the samples in VH McNutt Hall in room B30. The saw is to be set at 3800 RPM, at a rate of 0.10”/min, low force, and no rotation. Then once cutting procedures are completed, the samples, to obtain more accurate surface roughness features on the lattice structures, are to be polished using a Struers 74275 auto polisher. Making sure not to damage the lattices of the materials themselves. The following steps should be implemented for the auto polisher:

a) Ensure the water on the auto polisher is on and that a GECKO Pad is installed onto the auto polisher
b) Set the RPM to 300.
c) Make sure the auto polisher runs for 45 seconds.
d) Have the machine rotate in one direction only either clockwise or counterclockwise
e) Use a force of 100 Newtons for Stainless Steel and about 30 Newtons for Nylon to start
f) Keep the sample holder towards the edge of the rotating platform
g) Press the green button to start and the red button to stop on the machine.
h) Make sure to save the method onto the machine for later use.
i) Repeat steps a-I using grits papers (starting from 240 down to, 320, 600, and 800)

The recommended grits for griding are to be followed in order (Using Allied High Tech polishing paper).

a) 240 (50-10230)

b) 320 (50-10230)

c) 600 (20-10245)

d) 800 (20-10246)

### 3.4. IMAGE ACQUISITION

Then with the ground side up, the SEM (scanning electron microscope) and Hirox optical microscope are to be used at Straumanis – James Hall (See **Fig. (6)).** For the SEM, magnification factors of (x50, x200, x1000, x2500, x5000, and x10000) are to be implemented for the stainless steel and for nylon (x50, x100, and x100). Note that the sample must be lower than a certain height (roughly less than 0.75 in.) to fit into the SEM. For the Hirox optimal microscopes magnification factors of 2000 $\mu m$ and 500 $\mu m$ are to be set for nylon and stainless steel respectively at low-mid contrast settings, for best imaging results.


**Figure 6: SEM (left) and Hirox optical microscope (right)**

### 3.5. IMAGE ANALYSIS

Finally, after images from the SEM and optical microscopes are obtained for each material, the images deemed useful generated from either the optical microscope and or SEM are to be exported onto “ImageJ” and outlines of the structures can be generated by either automatically or manually (depending on user preference) the surface outlines of the nylon/steel materials, determine area using units of measurements determined by the user, and make approximations as to how much the area changes from a surface with surface roughness versus without surface roughness. In addition to a litany of other tools “Imagej” provides for surface roughness research purposes that can be further expanded upon in other research endeavors.

# 4. RESULTS AND DISCUSSION

The epoxy resin samples were successfully procured in the mounting cups of 1.5" diameters using the appropriate epoxy hardener mixture ratio. However, due to difficulties with the vacuum pump, the bubbles within the mixing cup could not be fully removed. Additionally, both the nylon and stainless-steel samples were both cleanly cut. However, the auto polisher at McNutt Hall could not be implemented due to the machine either being inactive or out of use. Lastly, both SEM and Hirox optical microscope images of the two sample types were taken and discussions on the images captured are to be discussed on **Sections 4.1-4.4**, ImageJ software analysis will be done within **Section 4.5** and correlations between results and the literature review will be detailed in **Section 4.6.** For both nylon and the stainless-steel samples, as expected, there are inherent surface roughness features seem on both materials

## 4.1. HIROX NON-METALLIC

For the non-metallics like nylon, they work very well utilizing Hirox microscopes. For instance, in **Fig. (7),** clear discontinuities can be seen within the lattice framework of the nylon material at a magnification of 2000 $\mu m$. More so on the interior of the material than on the outer boundaries. Further visualizations were improved upon using an open-source image software called PhotoKako, which marks clear boundaries on surface boundaries.

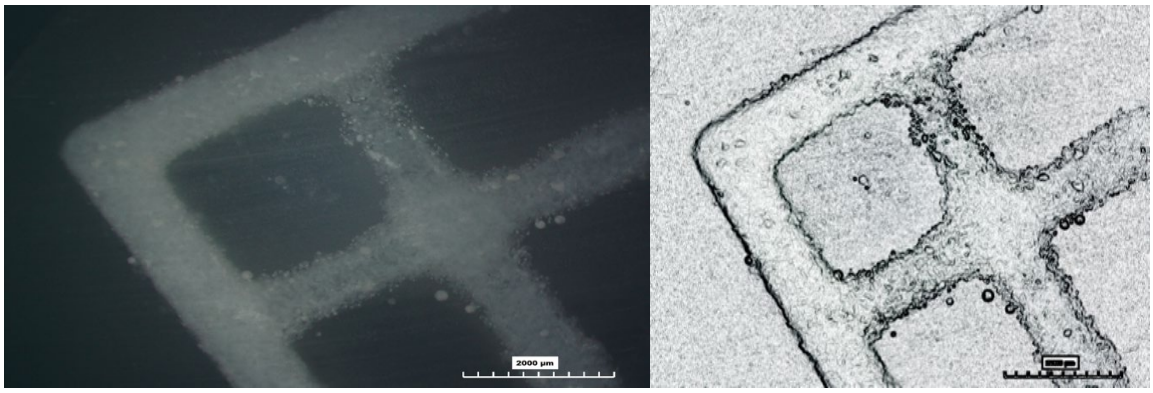


**Figure 7: Hirox Optical Microscope Images of Nylon Sample**

## 4.2. HIROX METALLIC

In addition to non-metals, metals like stainless steel well utilizing Hirox microscopes. As was seen in **Fig. (7)** for nonmetals, in **Fig. (8)** clear discontinuities can be seen within the circular branch lattice framework of the stainless-steel material and a large extrusion can be seen towards the left-hand side and right-hand side of the image at a magnification of 500 $\mu m$. Again, visualizations were improved upon using PhotoKako

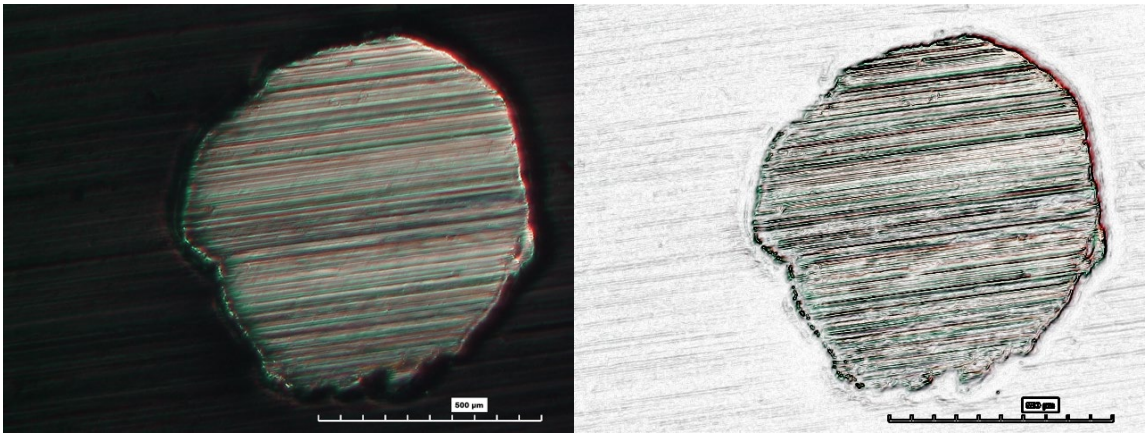


**Figure 8: Hirox Optical Microscope Images of Stainless-Steel Sample**

### 4.3. SEM NON-METALLIC

For the non-metallics like nylon, they do not work well utilizing SEM. As can be seen from **Fig. (9)** at a magnification of x50. It becomes very indiscernible to see the Nylon within the epoxy encapsulant. This is due the SEM only being apt for taking images of conductive materials like stainless steel or gold. As such, the nylon and would have to be coated with a thin layer of conductive material to see the structure of the material much more clearly. However, doing so would almost certainly change the surface roughness of the material itself. As such, for purposes of this research, only optical microscopes can be used for nonmetals.

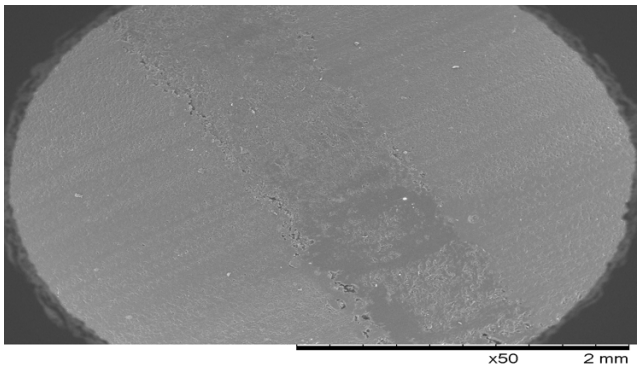


**Figure 9: SEM Image of Nylon Sample**

### 4.4. SEM METALLIC

However, SEM imaging is great for metals like stainless steel and discontinuities are very distinguishable (See **Fig. (10)**). With indentations clearly being seen on the right-hand side of the circular branch lattice structure at a magnification of 500 $\mu m$. In addition, extrusions can be seen on the top of the structure as well. Thus concluding, that for both nylon and stainless steel, there is an inherent level of surface roughness within each material

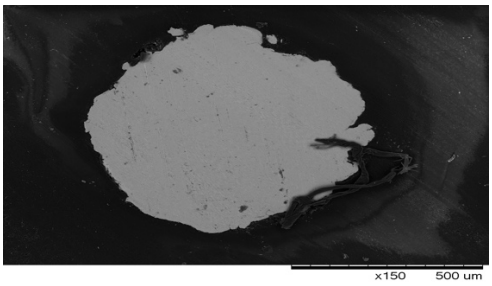


**Figure 10: SEM Image of Stainless-Steel Sample**

## 4.5. IMAGEJ SOFTWARE

From the ImageJ software, approximations into how much total surface area would be within the stainless-steel lattice structure based on this author's approximation of a circular lattice branch can be achieved. See **Fig. (11)** for yellow lines surrounding the stainless-steel structure to approximate the total surface area of the material. In comparison to approximating the total surface area of the Stainless-Steel sample with surface roughness (Area is equal to 46028320.312), the surface area is greater than that of the stainless-steel sample without surface roughness (Area is equal to 38640208.907). See **Fig. (12)** for details.

For the software to calculate the surface area, however, ImageJ asks for user defined unit of distance for reference. Both figures from the ImageJ software was approximated with micrometers ($\mu m$) as the base unit. This chosen distance was approximated based on the legend on the bottom right-hand corner of the optical microscope image taken for the stainless-steel sample.

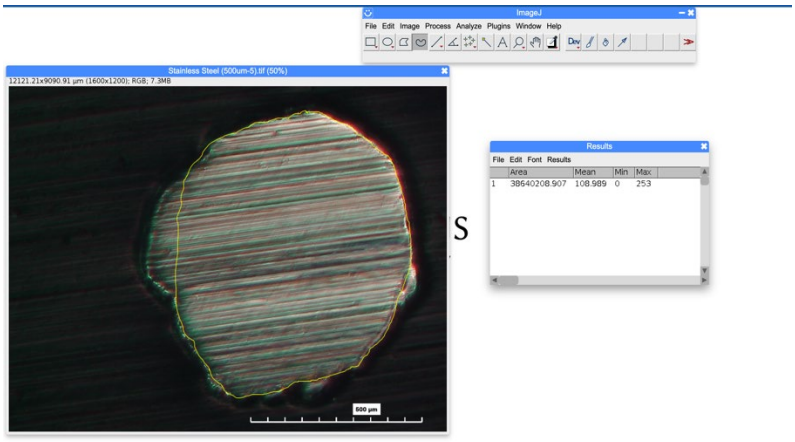

**Figure 11: ImageJ Image of Stainless-Steel Sample (Estimating Area without Surface Roughness)**

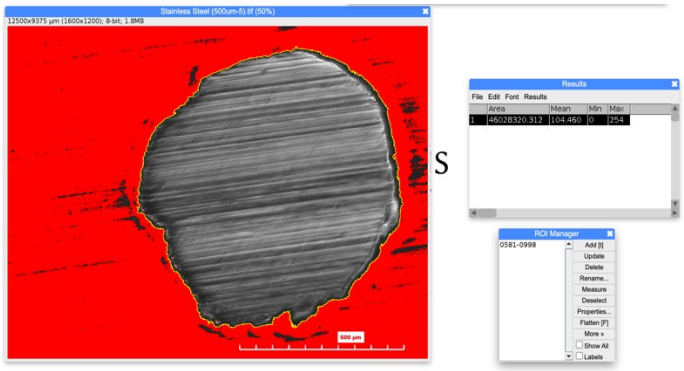

**Figure 12: ImageJ Image of Stainless-Steel Sample (Estimating Area with Surface Roughness)**

## 4.6. CORRELATIONS TO LITERATURE REVIEW

From the previous sets of images (**Figs. (11-12)),** some information can be analyzed from the experimental data and Literature Review. For starters, it is known that in an ideal case, the lattice structure should have very miniscule deviations into deviations of surface finish. However, in this experiment and especially in additive manufacturing, there is always going to be some uneven amount of surface roughness

associated with said products. Based on research from the *European Stainless Steel Development Association,* **Avi Leon**, and **Sacheva. Anish** it is very important to have smooth surfaces so that smooth operations can be performed in a variety of heat transfer systems, bearings, etc. As those with a rough surface finish cannot provide these features. Whether that decrease in surface quality comes from a lack of laser power in SLS processes, scan spacing, or an increase in the number of partially melted particles, a general lack of quality surface finish is not optimal for additive manufacturing.

In addition, an increase in surface roughness comes from an increased amount of surface area and protrusions on the stainless-steel surface from the SEM imaging. This will most likely lead to higher amounts of aerodynamic skin-friction drag and turbulence (**Rajappan, Anoop, et al and Ketut Aria Pria Utama, et. al**.)**.** Further compounding these trends is research performed by **Ehermann, Robert S., et.** al from Sandia National Laboratories where thicker airfoils grow more roughness sensitivity and hence maximum lift, drag ratio, lift-curve slope, and lift-to-drag ratio all decrease. Hence the larger the surface area, the larger and more numerous the surface area is, and the less efficient in general applications they become. This is especially true when the surface roughness has more peaks than pits with them (**Flack, K. A., et. al**).

# 5. SUMMARY AND RECOMMENDATIONS

In conclusion, experimental data collected from the nylon and stainless-steel lattice structures contained an inherent level of surface roughness at the finer scale, which aren't seen by the human eye. Surface Roughness can have a negative effect on additively manufactured materials and as such should be mitigated whenever possible. The area of the additively manufactured material tends to become greater whenever there is an inherent level of surface roughness as displayed for stainless steel. This increases the level of drag, skin friction, negative heat transfer/mass transfer properties, and other unwanted unsteady transitional flow characteristics. Though exceptions may exist for surface roughness either having very little adverse effects or improving flow characteristics such as those seen by **Barros, Julio M., et. al and Abbas, A. A., et al** seen in the literature review, all non-designed surface roughness should be mitigated as much as possible.

In addition, to further improve upon research on this topic for future researchers and honors academy members some additional steps should be taken. The vacuum chamber should be implemented so that all bubbles are removed from the epoxy resin sample and so there can be no misinterpretations on what is the lattice structure and what is a microbubble within the epoxy resin. Second, the surfaces of the material should be polished as outlined under the **Section 3.3** to provide a clear image on the SEM/optical microscope. Then the mixing cup diameter should be about 1.25" to fit onto the auto polishers more snuggly and to keep from debris entering the epoxy resin mixture

Lastly, an additional step in research should be implemented so that more analysis can be obtained on unsteady transitional flow characteristics. For instance, with constant

temperature anemometry (CTA) as used in measurements of turbulent gas flows. This is where a measure of turbulence in 1D, 2D, or 3D gases and liquid flows using hot-wire or hot-film probes are inserted into the flow This type of technology is highly useful fast fluctuations in flow to study flow of microstructures in which there is a need to resolve small flow eddies down to a tenth of a millimeter (**Danetic Dynamics**).

## REFERENCES


1. Leon, Avi, and Eli Aghion. "Effect of surface roughness on corrosion fatigue performance of AlSi10Mg alloy produced by Selective Laser Melting (SLM)." Materials Characterization 131 (2017): 188-194.
2. Sachdeva, Anish, Sharanjit Singh, and Vishal S. Sharma. "Investigating surface roughness of parts produced by SLS process." The International Journal of Advanced Manufacturing Technology 64.9-12 (2013): 1505-1516.
3. White Paper - Overcoming Additive Manufacturing Surface Finishing Challenges with Automated SRF Technologyhttps://manufacturing.report/Resources/Whitepapers/16052fd3-a544-471a-94dc-c114f29513ba_Overcoming-Additive-Manufacturing-Surface-Finishing-Challenges-with-Automated.pdf.
4. Calignano, Flaviana, et al. "Influence of process parameters on surface roughness of aluminum parts produced by DMLS." The International Journal of Advanced Manufacturing Technology 67.9-12 (2013): 2743-2751.
5. Udroiu, Razvan, Ion Cristian Braga, and Anisor Nedelcu. "Evaluating the quality surface performance of additive manufacturing systems: Methodology and a material jetting case study." Materials 12.6 (2019): 995.
6. European Stainless Steel Development Association. "Roughness Measurements of Stainless-Steel Surfaces." Union of International Associations, Brussels, Belgium (2014).
7. Strano, Giovanni, et al. "Surface roughness analysis, modelling and prediction in selective laser melting." Journal of Materials Processing Technology 213.4 (2013): 589-597.
8. Fox, Jason C., Shawn P. Moylan, and Brandon M. Lane. "Effect of process parameters on the surface roughness of overhanging structures in laser powder bed fusion additive manufacturing." Procedia Cirp 45 (2016): 131-134.
9. Townsend, Andrew, et al. "Surface texture metrology for metal additive manufacturing: a review." Precision Engineering 46 (2016): 34-47.
10. “Understanding Surface Finish in Metal 3d Printing - 3DEO - Metal Additive Manufacturing.” 3DEO, 18 Aug. 2020, https://www.3deo.co/metal-3d-printing/understanding-surface-finish-in-metal-3d-printing/.
11. Townsend, Andrew, et al. "Surface texture metrology for metal additive manufacturing: a review." Precision Engineering 46 (2016): 34-47.
12. Ehrmann, Robert S., et al. Effect of Surface Roughness on Wind Turbine Performance. No. SAND2017-10669. Sandia National Lab.(SNL-NM), Albuquerque, NM (United States), 2017.
13. Rajappan, Anoop, et al. "Influence of textural statistics on drag reduction by scalable, randomly rough superhydrophobic surfaces in turbulent flow." Physics of Fluids 31.4 (2019): 042107.
14. Barros, Julio M., Michael P. Schultz, and Karen A. Flack. "Measurements of skin-friction of systematically generated surface roughness." International Journal of Heat and Fluid Flow 72 (2018): 1-7.
15. Flack, Karen A., and Michael P. Schultz. "Roughness effects on wall-bounded turbulent flows." Physics of Fluids 26.10 (2014): 101305.

16. Skin Friction Measurements of Systematically Varied Roughness: Probing the Role of Roughness Amplitude and Skewness
17. Abbas, A. A., et al. "Surface roughness effects on turbulent boundary layer structure of NACA 0026 Airfoil." International Journal of Engineering & Technology 7.3.17 (2018): 254-259.
18. Harun, Zambri, et al. "Surface roughness effects studies in transportation industries." Jurnal Kejuruteraan SI 1.7 (2018): 87-90.
19. Flack, Karen A., Michael P. Schultz, and Ralph J. Volino. "The effect of a systematic change in surface roughness skewness on turbulence and drag." International Journal of Heat and Fluid Flow 85 (2020): 108669
20. “Constant Temperature Anemometry (CTA): Thermal Anemometer.” *Dantec Dynamics | Precision Measurement Systems & Sensors*, 25 Feb. 2022, https://www.dantecdynamics.com/solutions-applications/solutions/fluid-mechanics/constant-temperature-anemometry-cta/#:~:text=Constant%20Temperature%20Anemometry%20(CTA)%2C,probes%20inserted%20into%20the%20flow.
21. Hakim, Muhammad Luqman, et al. “Drag Penalty Causing from the Roughness of Recently Cleaned and Painted Ship Hull Using RANS CFD.” *CFD Letters*, vol. 12, no. 3, 2020, pp. 78–88., https://doi.org/10.37934/cfdl.12.3.7888.